MEASUREMENT OF THE TRANSVERSE BEAM DYNAMICS IN A TESLA-TYPE SUPERCONDUCTING CAVITY*

A. Halavanau[1,2], N. Eddy[2], D. Edstrom[2], A. Lunin[2], P. Piot[1,2], J. Ruan[2], N. Solyak[2]
[1] Department of Physics and Northern Illinois Center for Accelerator & Detector Development, Northern Illinois University, DeKalb, IL 60115, USA
[2] Fermi National Accelerator Laboratory, Batavia, IL 60510, USA

Abstract

Superconducting linacs are capable of producing intense, ultra-stable, high-quality electron beams that have widespread applications in Science and Industry. Many project are based on the 1.3-GHz TESLA-type superconducting cavity. In this paper we provide an update on a recent experiment aimed at measuring the transfer matrix of a TESLA cavity at the Fermilab Accelerator Science and Technology (FAST) facility. The results are discussed and compared with analytical and numerical simulations.

INTRODUCTION

Several projects are foreseen to incorporate TESLA-type cavities [1, 2]. These include electron- [3], muon- [4], and proton-beam accelerators [5]. The transverse beam dynamics associated to these accelerating cavities has been explored in the last decade [6, 7]. Recently, we attempted to characterize the transfer matrix associated to a TESLA cavity and some preliminary measurement were reported in Ref. [8]. In this paper we improve our previous measurement and confirm that the measured transfer matrix is well described by the by Chambers' [9] model. We especially find that the inclusion of spatial harmonics as discussed in [10–14] is not relevant for the TESLA cavity.

In brief, we consider the transfer matrix R of the cavity in the transverse trace space to be defined as $\mathbf{x}_f = R\mathbf{x}_i$ where $\mathbf{x} \equiv (x, x')$ and the subscript i (resp. f) corresponds to the coordinates upstream (resp. downstream) of the cavity. According to the Chambers' model, the elements of 2×2 matrix R are [9, 12–14]:

$$\begin{aligned} R_{11} &= \cos\alpha - \sqrt{2}\cos(\Delta\phi)\sin\alpha, \\ R_{12} &= \sqrt{8}\frac{\gamma_i}{\gamma'}\cos(\Delta\phi)\sin\alpha, \\ R_{21} &= -\frac{\gamma'}{\gamma_f}\left[\frac{\cos(\Delta\phi)}{\sqrt{2}} + \frac{1}{\sqrt{8}\cos(\Delta\phi)}\right]\sin\alpha, \quad (1) \\ R_{22} &= \frac{\gamma_i}{\gamma_f}[\cos\alpha + \sqrt{2}\cos(\Delta\phi)\sin\alpha], \end{aligned}$$

where $\alpha \equiv \frac{1}{\sqrt{8}\cos(\Delta\phi)} \ln\frac{\gamma_f}{\gamma_i}$, $\gamma_f \equiv \gamma_i + \gamma' z$ is the final Lorentz factor, and $|R| = \gamma_i/\gamma_f$.

The analytical solution (1) is obtained under the assumption of axially symmetric field. It is not the case in a real RF cavity which includes input-power and high-order-mode (HOM) couplers needed to respectively couple the RF power to the cavity and damp the HOM fields excited by the beam.

To investigate the impact of couplers further, a 3D electromagnetic model of the cavity − including its auxiliary couplers − was implemented in HFSS [15]. The simulated 3D electromagnetic field map was imported in ASTRA [16] particle-tracking program. The map was computed over a the domain $x = y = \pm 10$ mm from the cavity axis and over $z = 1395$ mm along the cavity length. The respective mesh size were taken to be $\delta x = \delta y = 0.5$ mm and $\delta z = 1$ mm. In our previous studies it was found, via numerical simulation, that the main effect of the 3D model is to induce some beam steering. However, we did not find significant deviations in the cavity transverse-focusing properties from the 1D (i.e. without including 3D effect) model. In particular, simulations indicated a good agreement of the transverse focusing with the analytical model from Chambers [8].

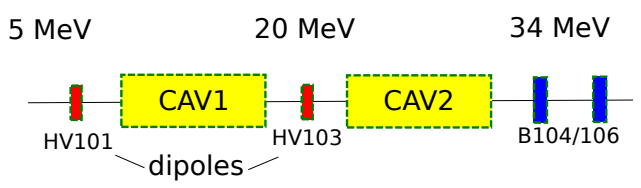

Figure 1: Experimental setup under consideration: two SRF-cavities(CAV1/CAV2) and beam position monitors (BPM 104/106) used in measurements.

EXPERIMENTAL SETUP & METHOD

The experiment was performed at the FAST injector [17] and is the continuation of studies performed earlier at Fermilab A0 photoinjector facility [6] and FAST facility [8]. A significant change from our previous experiment was the addition of a second cavity and the modification of some of the diagnostics.

In brief, an electron beam photoemitted from a high-quantum efficiency is rapidly accelerated to 5 MeV in a L-band RF gun. The beam is then injected in TESLA cavity (CAV1) with average accelerating gradient limited to $\bar{G}_{rf} \simeq 15$ MeV/m and further accelerated to a maximum energy of ~ 34 MeV in the second cavity (CAV2); Fig. 1.)

A priori to performing the experiment, a beam-based alignment through both cavities was performed. The procedure was accomplished using a conjugate gradient algorithm available within SCIPY library and using PyACL framework [18]. In order to measure the transfer matrix, beam-

* This work was supported by the US Department of Energy under contract DE-SC0011831 with Northern Illinois University. Fermilab is operated by the Fermi research alliance LLC under US DOE contract DE-AC02-07CH11359.

trajectory perturbations were applied via small kicks using horizontal and vertical steerers located upstream of CAV2. In our experiment, a set of 20 dipole kicks (see Fig. 1) were randomly applied to ensure full beam transmission and to populate transverse (x, x', y, y') centroid trace space such that it had significant statistical volume.

The beam was then propagated through CAV2 up to a pair of electromagnetic button-style beam position monitors (BPMs) located downstream. The measurement of beam position with CAV2 "off" and "on" (indirectly) provided the input $\mathbf{X_i}$ and final $\mathbf{X_f}$ beam positions and divergences [here $\mathbf{X} \equiv (x, x')^T$] respectively upstream and downstream of CAV2.

Correspondingly, given the transfer matrix of the cavity R, we have $\mathbf{X_f} = R\mathbf{X_i}$. Consider $\mathbf{X_{0_i}}$ to be some reference orbit, so that we can rewrite the transformation as $\mathbf{X_f} = R(\mathbf{X_{0_i}} + \Delta\mathbf{X_{0_i}})$. It immediately follows that $R(\mathbf{X_{0_i}} + \Delta\mathbf{X_{0_i}}) = \mathbf{X_{0_f}} + \Delta\mathbf{X_{0_f}}$ and therefore $\Delta\mathbf{X_{0_f}} = R\Delta\mathbf{X_{0_i}}$. So any selected orbit can serve as a reference orbit to find the transformation R, assuming the set of perturbed trajectories around this reference is transformed linearly (which is the essence of the paraxial approximation). Impressing a set of N perturbations results in a system of N equations of the form $\Xi_f = R\Xi_i$ where Ξ_j $(j = i, f)$ are $2 \times N$ matrices containing the positions and divergence associated to the N perturbations. This system is inverted via a least-square technique to recover R. The method can be further extended to the transverse 4D phase space to yield the 4×4 transfer matrix of the cavity.

TRANSFER MATRIX

The measurements were made for 7 phases in a range of [-20,20] degrees. Each time $\sim$ 80 trajectories were stored corresponding to 20 different orbit settings recorded 4 times to average over beam-position jitter (both physical and instrumental) and provide statistical error bars. The comparison of the recovered transfer matrix elements with the Chambers' model and the one derived from particle tracking with ASTRA in the 3D field map are presented in Figs. 2,3.

First, it should be noted that the slight discrepancies between the Chambers' model and the particle tracking results are attributed to the instrumental jitter of the BPMs of ≈ 80 μm, and RF-calibration uncertainty.

Overall we observe an excellent agreement between experiment and the models for the 2×2 diagonal blocks of the experimental transfer matrix; see Fig. 2. All the matrix elements agree within the calculated error bars with the measured accelerating phase $\phi \in [-20, 20]^\circ$. During the measurement we were unable to set the phase of the CAV2 beyond the aforementioned range as it would require a significant reconfiguration of the FAST beamline.

The coupling (anti-diagonal) 2×2 blocks modeled by the simulation are very small and seem to be corroborated with our experimental results; see Fig. 2. The latter observation indicates that for the range of parameters being explored the 3D effects associated to the presence of the couplers appear

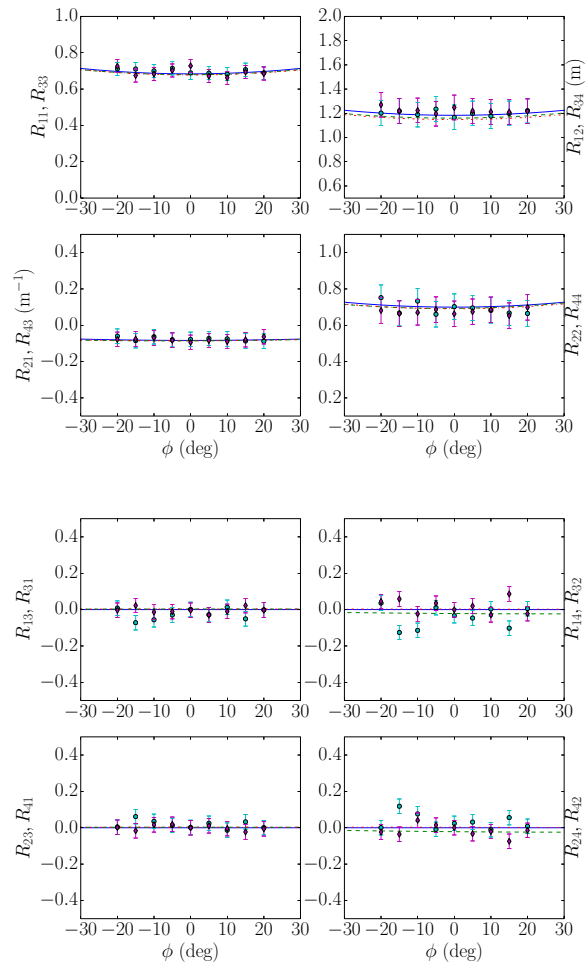

Figure 2: Main diagonal and anti-diagnonal blocks of the transport matrix. The solid (blue) lines represent Chambers' approximation, dashed (green/red) lines are obtained from 3D field map simulations for (x, x') and (y, y') planes respectively, circular markers and purple lozenges correspond to experimental values for (x, x') and (y, y') planes respectively.

to have a very small effect on the beam dynamics. Finally, we find that determinant $|R|$ is consistent within the error bars with simulations; see also [6].

COUPLER & 3D EFFECTS

The measurements presented in Figs. 2,3 suggest that HOM coupler effect can be viewed within the error bars as an additional phase dependent dipole field inside the cavity. In order to study this effect, we performed a wide range phase-scan of the CAV2 with CAV1 "on". 5 trajectories were recorded and averaged in order to mitigate possible ponderomotive steering introduced by the cavity via misalignment errors.

The resulting average trajectory in both transverse planes is shown in Fig. 4. As one can infer from Fig. 4 the HOM coupler response is asymmetric with phase. It also illustrates

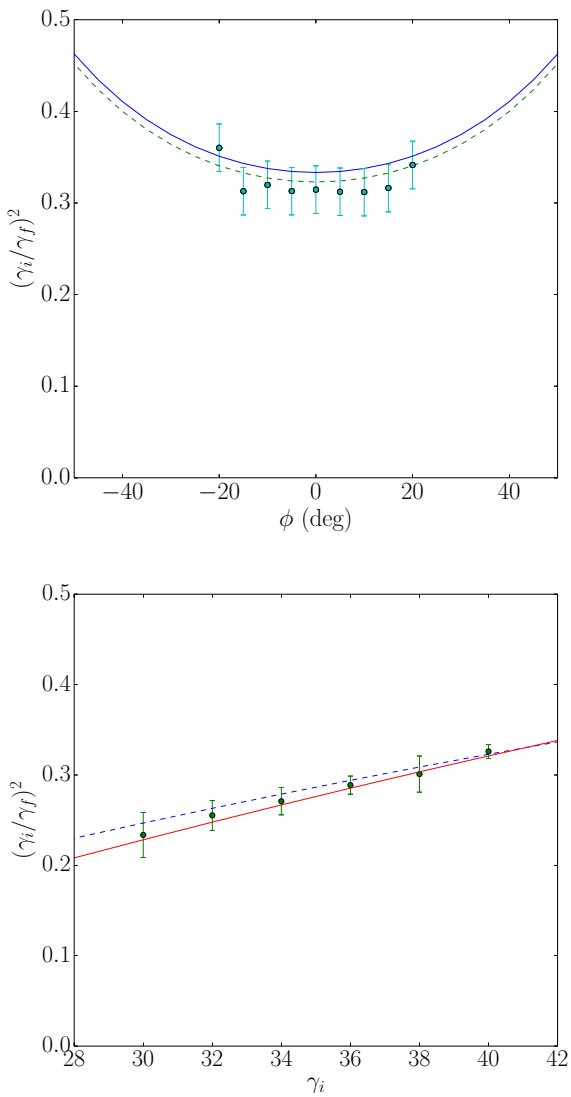

Figure 3: (top) 4×4 transfer matrix determinant, calculated in Chambers' approximation (blue line), 3D field map simulations (dashed line) and experimentally measured values (circular markers). (bottom) The demonstration of matrix determinant damping with the varying incoming beam energy. Dashed line corresponds to Chambers' approximation and solid line represents numerical simulations.

that TESLA-type cavity alignment is non-trivial and can not be done by pure model beam-based alignment. The most accurate way of aligning the beam through a TESLA-type cavity is to ensure the minimization of the HOM-modes via HOM-pickup device. Such a study is ongoing at FAST. This data will be further analyzed via numerical simulations and will be reported elsewhere.

SUMMARY

We reported the results of the measurement of the transfer matrix of a TESLA-type cavity at FAST. The minimizing algorithm was used for beam-based alignment in both RF-

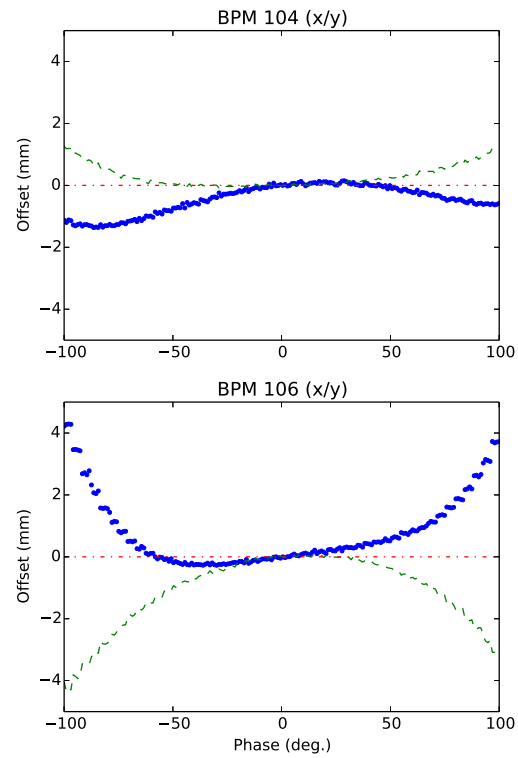

Figure 4: HOM coupler response at different cavity phases seen on BPM104/BPM106. Dashed/circular markers represent X/Y trajectories respectively. Red dotted line is drawn for the reference.

cavities. Despite some technical limitations, the presented measurements are consistent with the results from 3D field map simulations and analytical prediction. The HOM coupler doesn't affect the transverse matrix within the errorbars and can be considered as a phase-dependent dipole kick in the cavity. The experiment motivated the development of a PYTHON-based accelerator control framework that will be described elsewhere [18].

REFERENCES

[1] S. Fartoukh, *Report TESLA* 98-01, DESY (1998).

[2] B. Aunes *et al.*, *Phys. Rev. ST Accel. Beams* **3**, 092001(2000).

[3] A. Vivoli *et al.*, "Lcls-ii injector coupler options performance", technical note LCLS-II TN-15-03 (2015).

[4] M. Popovic and R.P. Johnson, *Nucl. Phys. Proc. Suppl.*, **155**, 305, (2006).

[5] S. Holmes *et al.*, in *Proc. of IPAC'15*, paper THPF116, (2015).

[6] P. Piot and Y.E. Sun, "Note on the transfer matrix measurement of a tesla cavity", *Report Beams Document* 1521-v1, Fermilab (2004).

[7] P. Piot *et al.*, "Steering and focusing effects in TESLA cavity due to high order mode and input couplers", *Conf. Proc.*, C0505161:4135 (2005).

[8] A. Halavanau *et al.*, in *Proc. of IPAC'16*, paper TUPMY038, (2016).

[9] E. E. Chambers, "Radial transformation matrix, standing wave accelerator", *HEPL* TN-68-17 and *HEPL* 570 (Oct. 1968).

[10] S. Reiche *et al.*, "Experimental confirmation of transverse focusing and adiabatic damping in a standing wave linear accelerator", *Phys. Rev.*, **E56**, 3572 (1997).

[11] Yu. Eidelman *et al.*, "A new approach to calculate the transport matrix in RF cavities", *Conf. Proc.*, C110328:1725 (2011).

[12] J. Rosenzweig and L. Serafini, "Transverse particle motion in radiofrequency linear accelerators", *Phys. Rev.*, **E49**, 1599 (1994).

[13] S. C. Hartman and J. B. Rosenzweig, "Ponderomotive focusing in axisymmetric rf linacs", *Phys. Rev.*, **E47**, 2031 (1993).

[14] S. C. Hartman, Phd thesis. *UCLA* (1994).

[15] *High Frequency Structure Simulator* software available from ANSYS.

[16] K. Flöttmann, *ASTRA reference manual*, DESY (2000).

[17] E. Harms *et al.*, *ICFA Beam Dyn. Newslett.*, **64** 133 (2014).

[18] P. Piot and A. Halavanau, to be presented at NAPAC16, Chicago, USA, paper TUPOA48, (2016).